Effect of Capping Structure on the High Temperature Annealing of GaN

Jordan D. Greenlee[1], Boris N. Feigelson[2], Jennifer K. Hite[2], Karl D. Hobart[2], Francis J. Kub[2], Travis J. Anderson[2]

[1]National Research Council Postdoctoral Fellow residing at U.S. Naval Research Laboratory, 4555 Overlook Ave. SW Washington, DC 20375, USA, [2]Naval Research Laboratory 4555 Overlook Ave. SW Washington, DC 20375, USA

E-mail: jordan.greenlee.ctr@nrl.navy.mil

Keywords: GaN, Ion Implantation, Annealing, Raman spectroscopy

Abstract

Two capping structures for protection of GaN during high temperature annealing were compared, a dual-layer MOCVD grown cap and a dual-layer MOCVD + sputtered cap. It was determined that adding a 250 nm sputtered AlN layer on top of the dual layer MOCVD grown AlN cap resulted in a significantly better capping structure. The capping efficacy was quantified using Nomarski optical microscope images and Raman spectroscopy before and after a 1500 ˚C pulse. GaN capped with the sputtered AlN had fewer pits on the surface and an improved crystalline quality as determined by Raman spectroscopy analysis.

INTRODUCTION

GaN and its alloys have been widely researched due to their wide range of advantageous properties and potential applications. The Baliga figure of merit for GaN is higher than that of other materials such as Si and SiC, making it well suited for power electronic applications [1]. The III-nitride system also has a tunable direct bandgap from 0.7 to 6.1 eV, making it well suited for optoelectronic applications [2]. III-nitride materials are also a promising radiation hard material for use in space and military environments [3].

Despite having advantages compared to other candidate power materials, the processing technology of GaN has not reached the same level of maturity as that of its competitors. This lack of advanced processing technology, in particular planar processing, is one of the critical limiting factors in the widespread use and adoption of GaN. One specific area of processing which has been a major limitation for GaN is the implantation and activation of p-type dopants.

The ability to implant and activate p-type dopants will enable many devices, including vertical device structures like the current aperture vertical electron transistor (CAVET) [4]. Several researchers have tried to implant Mg and anneal GaN at high temperatures and high pressures to activate implanted Mg, but success has been limited in obtaining p-type conduction [5]. Some have had success in co-implanting Mg with N, but this requires an extra implantation step and introduces more damage in the crystalline lattice, which then must be repaired in the annealing process [6].

MULTICYCLE RAPID THERMAL ANNEALING

The most successful method of activating implanted Mg in GaN is via the multicycle rapid thermal annealing (MRTA) process [7]. Activation of Mg of up to ~8% has been achieved using the MRTA process [8]. There are four components to the MRTA process. First, a considerable nitrogen overpressure of 24 bar is used to increase the decomposition temperature of GaN. This pressure is high enough to maintain the thermodynamic stability of GaN up to temperatures of about 975 ˚C [7].

The second component of the MRTA process is a conventional anneal that is conducted at a thermodynamically stable temperature on the order of tens of minutes. This conventional anneal is performed before the implanted sample is subjected to higher temperatures to partially recover the damage created during ion implantation. It was previously shown that conventional anneals at about 1150 ˚C are an ideal balance for preserving the surface structure while repairing crystalline damage [9]. It was also shown that the conventional annealing step is a critical step in the MRTA process, and failure to implement this step will result in severely damaged GaN [10].

Rapid heating and cooling pulses are the third key component of the MRTA process. The rapid pulses are kept short enough to avoid GaN decomposition. The total integrated time that the GaN is subjected to higher temperature is increased by repeated pulsing.

The fourth key feature of the MRTA process is the use of an AlN cap. Capping structures have been previously shown to prevent GaN decomposition at otherwise thermodynamically unstable conditions [11]. Several capping materials have been utilized in the past with AlN giving the best results [12]. Both sputtered and MOCVD-based AlN have been utilized [13]. Originally, a two-layer MOCVD cap was utilized in the MRTA process to avoid GaN decomposition [7]. The cap consists of a thin (~4 nm) AlN grown at 1100 ˚C. This layer is utilized to provide a high quality interface between the GaN and AlN and kept thin to avoid exceeding the critical thickness of AlN on GaN. A thicker (25 nm) AlN layer is then grown at a lower

temperature on top of the high temperature AlN layer as shown in Fig. 1a. This thicker AlN is used as mechanical support for the thinner high quality AlN. In this research, we investigate an additional sputtered layer on top of the dual layer MOCVD cap as shown in Fig. 1b to provide additional mechanical support for the capping structure.

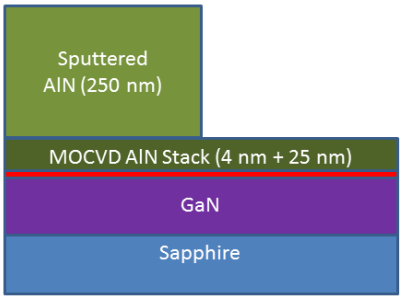

Figure 1. Schematic of AlN capped GaN structures used in this research. The sample is capped with MOCVD AlN only on half of the sample and a combination of MOCVD and sputtered AlN on the second half.

EXPERIMENTAL

The GaN used in this study was grown in a Thomas Swan MOCVD reactor on an a-plane sapphire substrate and was 2.0 µm thick. The two MOCVD AlN capping layers were grown on the GaN layer, with the thin 4 nm layer grown at 1100 ˚C and the thicker 25 nm layer grown subsequently at 600 ˚C. The sample was then implanted with the conditions shown in Table I. The implantation doses and energies were chosen such that there would be an Mg concentration of ~10^{19}/cm^3 up to 500 nm deep in the GaN film.

After implantation, the capped GaN was annealed with a 30 minute conventional anneal at 1140 ˚C to repair some of the implantation damage. After the conventional anneal, the sample was annealed with a 1500 ˚C pulse. This annealing temperature is significantly higher than previously used in the MRTA process to activate implanted Mg, but was chosen to stress the cap and obtain surface damage thereby allowing for a comparison of the efficacy of the additional sputtered AlN in the capping structure. After annealing, the samples were removed from the chamber and etched in AZ400K, a selective AlN wet etchant, to expose the GaN surface [14,15].

TABLE I
MG IMPLANTATION SCHEDULE

Mg Energy (keV)	Dose (cm^{-2})
50	5.0 x 10^{13}
140	1.1 x 10^{14}
300	3.0 x 10^{14}

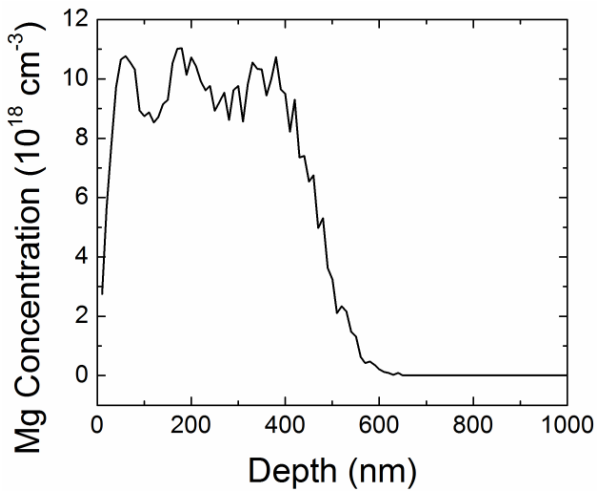

Figure 2. Implantation profile used in this experiment. Doses and energies were chosen to assure Mg concentrations of ~10^{19}/cm^3 up to 500 nm deep in the GaN film.

Samples were characterized using Raman Spectroscopy using a Thermo Scientific DXR Raman Microscope with a 532 nm laser at 4.0 mW of power. The surface morphology was characterized using Nomarski optical microscroscopy.

RESULTS AND DISCUSSION

After sputtering and before annealing, Nomarski optical imaging was used to inspect the surface of the sample. Figure 3 shows the sample surface at the dividing line between the MOCVD + Sputtered AlN (Left) and MOCVD AlN (Right). No immediate differences in surface morphology before annealing can be discerned.

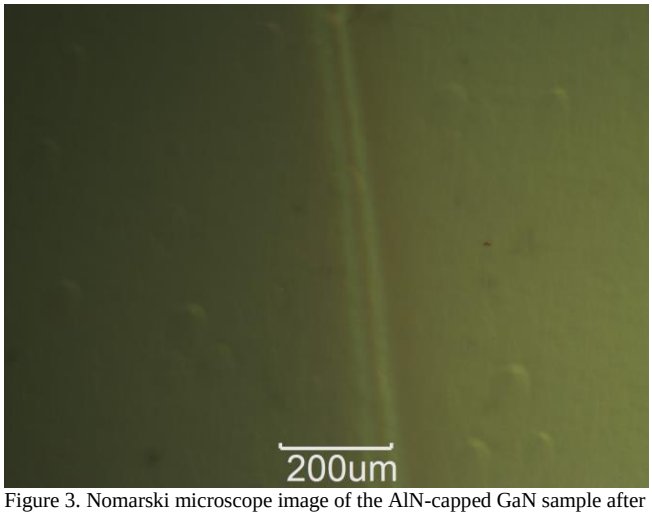

Figure 3. Nomarski microscope image of the AlN-capped GaN sample after implantation and sputtering. The left side of the vertical line is protected by both MOCVD and sputtered AlN while the right side of the sample is protected by only MOCVD-grown AlN.

After annealing, the AlN cap was etched in an AlN selective wet etchant, AZ400K. Previously, AZ400K has been shown to be selective for AlN over GaN without

causing surface damage [15]. The GaN surface is shown in Figure 4. The back of the sample was scribed to signify the line between the side that received a sputtered AlN cap and the side that did not. On the right of the vertical scribe line in Figure 4, the surface was not protected by sputtered AlN, and clearly exhibits damage. The surface unprotected by sputtered AlN has a large density of etch pits, presumably caused by thermal decomposition of the GaN during the 1500 ˚C thermal pulse. The density of etch pits was determined to be 1518/mm^2 for the side of the sample that was not protected by sputtered AlN. In comparison, the side that was protected by 250 nm of sputtered AlN only had 9 etch pits/mm^2, clearly indicating that the capping structure that includes both sputtered and MOCVD-grown AlN improves the thermal resilience of the underlying GaN compared to the capping structure that consists of MOCVD-grown AlN alone.

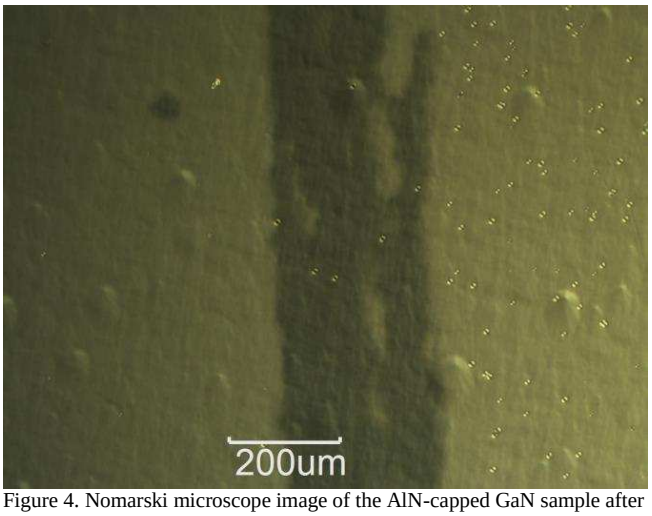

Figure 4. Nomarski microscope image of the AlN-capped GaN sample after annealing and etching the AlN capping layers. A vertical line was scribed in the back of the sample prior to etching the AlN to denote the dividing line between the sputtered portion and unsputtered portion of the sample. The left side of the vertical line was protected by both MOCVD and sputtered AlN while the right side of the sample was protected by only MOCVD-grown AlN. The sputtered side of the sample clearly has less thermal etch pits due to enhanced thermal decomposition protection with the thicker AlN layer.

Raman spectroscopy was utilized to determine structural changes during the annealing process on both the sputter-capped side of the sample and the side of the sample not protected by sputtered AlN. Spectra from both the as-implanted and post-annealed states of the sample are shown in Figure 5. As implanted, the Raman spectra has additional peaks coinciding with crystal damage modes (atomic vacancies and interstitials) [16]. However, after annealing, the damage modes have largely disappeared, leaving the GaN E_2 and A_1 (LO) modes at 570 cm^{-1} and 730 cm^{-1}, respectively. This removal of the damage modes indicates that the crystal has significantly improved through the annealing process. To quantify and compare the crystalline improvement, the E_2 full width at half-maximum (FWHM) was compared. After implantation, the FWHM was 6.47 cm^{-1}. After annealing, the FWHM of spectra taken in the sputter-capped portion of the sample is 3.09 cm^{-1} while the FWHM of the area of the sample without the sputtered cap is 3.21 cm^{-1} as shown in Figure 6. A decrease in the FWHM indicates an increase in the crystalline quality, so both portions of the sample after annealing have drastically improved compared to the as-implanted sample. The portion of the sample that had the combined MOCVD and sputtered cap had a higher crystal quality compared to the portion of the sample with the MOCVD cap alone.

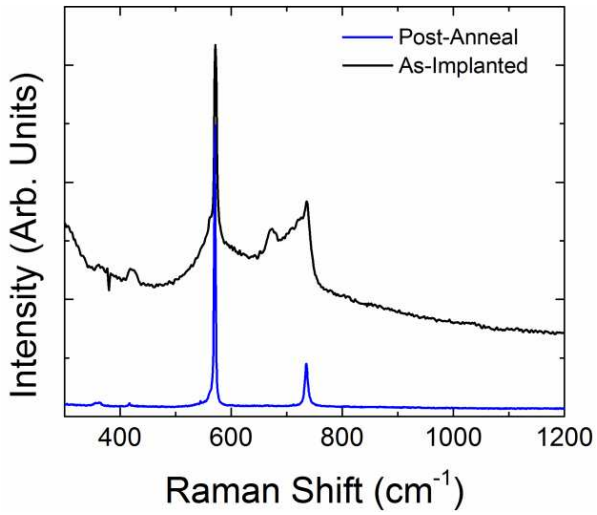

Figure 5. Raman spectra of as-implanted and post-annealed GaN. After annealing, the peaks corresponding with damage disappear.

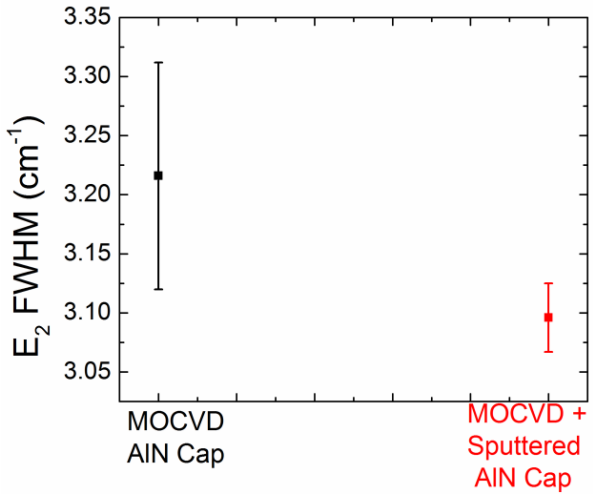

Figure 6. The Raman E_2 mode FWHM of the GaN in the sputtered and unsputtered portions of the sample. The GaN protected by the sputtered cap has a lower FWHM, indicating a better crystalline quality.

CONCLUSIONS

In conclusion, two capping structures were compared, a dual-layer MOCVD grown cap and a dual-layer MOCVD +

sputtered cap. It was determined that adding a 250 nm sputtered AlN to the MOCVD grown AlN cap resulted in a significantly better capping structure and improved the thermal resilience of the annealing process. This was determined by Nomarski optical microscope images and Raman spectroscopy before and after a 1500 ˚C pulse. GaN capped with MOCVD and sputtered AlN had fewer pits on the surface and had an improved crystalline quality compared to the side of the sample without sputtered AlN. This MOCVD + sputtered AlN capping structure will enable high temperature processing of GaN, including selective area dopant activation for advanced power devices.

ACKNOWLEDGEMENTS

This research was performed while J. D. Greenlee held a National Research Council Research Associateship Award at the Naval Research Laboratory. Research at NRL was supported by the Office of Naval Research.

ACRONYMS

MRTA: Multicycle Rapid Thermal Annealing
FWHM: Full Width at Half Maximum

REFERENCES

[1] T. P. Chow and R. Tyagi, IEEE Trans. Elec. Dev. **41,** 1481 (1994).
[2] E. Matioli, C. Neufeld, M. Iza, S. Cruz, A. A. Al-Heji, X. Chen, R. M. Farrell, S. Keller, S. DenBaars, U. Mishra, S. Nakamura, J. Speck, and C. Weisbuch, Appl. Phys. Lett. **98,** 021102 (2011).
[3] T. J. Anderson, A. D. Koehler, J. D. Greenlee, B. D. Weaver, M. A. Mastro, J. K. Hite, J. C. R. Eddy, F. J. Kub, and K. D. Hobart, IEEE Electron Device Lett. **35,** 826 (2014).
[4] S. Chowdhury, B. L. Swenson, and U. K. Mishra, IEEE Electr. Device Lett. **29,** 543 (2008).
[5] M. Kuball, J. M. Hayes, T. Suski, J. Jun, M. Leszczynski, J. Domagala, H. H. Tan, J. S. Williams, and C. Jagadish, J. Appl. Phys. **87,** 2736 (2000).
[6] K. T. Liu, Y. K. Su, S. J. Chang, and Y. Horikoshi, J. Appl. Phys. **98,** 073702 (2005).
[7] B. N. Feigelson, T. J. Anderson, M. Abraham, J. A. Freitas, J. K. Hite, C. R. Eddy, and F. J. Kub, J. Cryst. Growth **350,** 21 (2012).
[8] T. J. Anderson, B. N. Feigelson, F. J. Kub, M. J. Tadjer, K. D. Hobart, M. A. Mastro, J. K. Hite, and C. R. E. Jr., Electronics Lett. **50,** 197 (2014).
[9] J. D. Greenlee, B. N. Feigelson, T. J. Anderson, M. J. Tadjer, J. K. Hite, M. A. Mastro, C. R. Eddy, K. D. Hobart, and F. J. Kub, J. Appl. Phys. **116** (2014).
[10] J. D. Greenlee, B. N. Feigelson, T. J. Anderson, M. J. Tadjer, J. K. Hite, C. R. Eddy, K. D. Hobart, and F. J. Kub, in Process optimization of multicycle rapid thermal annealing of Mg-implanted GaN, 2014 IEEE Workshop on Wide Bandgap Power Devices and Applications (WiPDA), p. 59.
[11] J. C. Zolper, D. J. Rieger, A. G. Baca, S. J. Pearton, J. W. Lee, and R. A. Stall, Appl. Phys. Lett. **69,** 538 (1996).
[12] G. S. Siddarth, M. Madhu, V. R. Mulpuri, A. S. John, M. A. Mastro, R. E. Charles, Jr., R. T. Holm, R. L. Henry, A. F. Jaime, Jr., G.-N. Elba, R. D. Vispute, and T. Yong-Lai, Semicond. Sci. Technol. **22,** 1151 (2007).
[13] C. E. Hager, K. A. Jones, M. A. Derenge, and T. S. Zheleva, J. Appl. Phys. **105,** 033713 (2009).
[14] J. R. Mileham, S. J. Pearton, C. R. Abernathy, J. D. MacKenzie, R. J. Shul, and S. P. Kilcoyne, Appl. Phys. Lett. **67,** 1119 (1995).
[15] J. D. Greenlee, T. J. Anderson, B. N. Feigelson, A. D. Koehler, K. D. Hobart, and F. J. Kub, Appl. Phys. Express **8,** 036501 (2015).
[16] M. Katsikini, K. Papagelis, E. C. Paloura, and S. Ves, J. Appl. Phys. **94,** 4389 (2003).